Supplemental materials

Figure S1

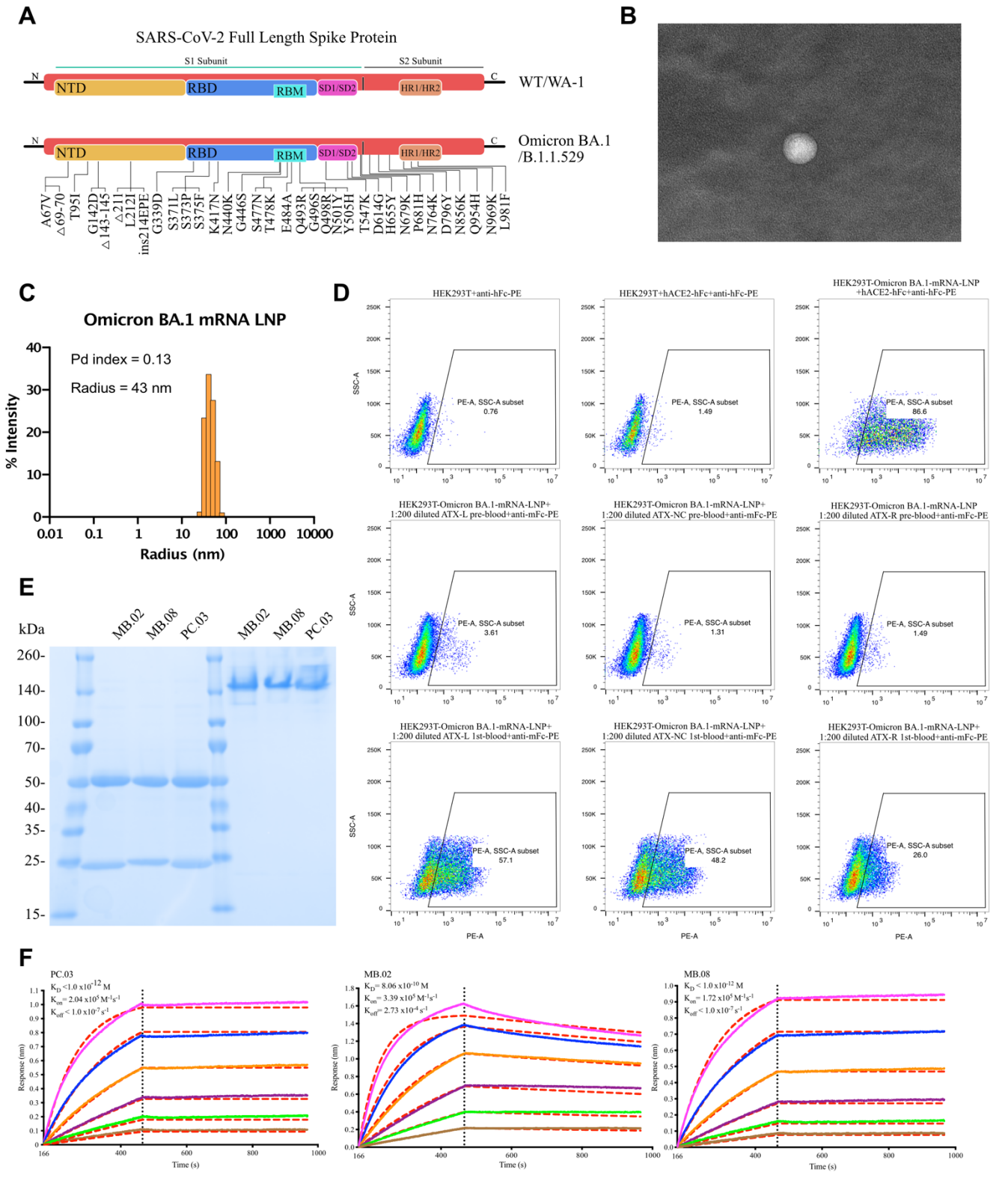

Figure S1. Characterization of Omicron BA.1-spike specific LNP-mRNAs, and biophysics of leading antibody clones, Related to Figures 1 and 2

A, Schematic showing the domain arrangement of the SARS-CoV-2 WT spike and its recent variant SARS-CoV-2 B.1.1.529 (Omicron BA.1). Mutations present in Omicron spike protein are labeled. Full-length Omicron BA.1spike gene was synthesized to construct Omicron BA.1-specific mRNA-lipid nanoparticle and Omicron BA.1-specific pseudo-virus.

B, Omicron BA.1 LNP-mRNA image collected on transmission electron microscope.

C, Dynamic light scattering derived histogram depicting the particle radius distribution of Omicron BA.1 spike LNP-mRNAs

D, Human ACE2 receptor binding of Omicron BA.1 spike expressed in HEK293T cells as detected by human ACE2-Fc fusion protein and PE-anti-human Fc antibody on flow cytometry.

E, SDS-PAGE analysis of purified mAbs under nonreducing and reducing (10mM DTT) conditions. Four micrograms of purified protein were analyzed using a Novex WedgeWell 4-20% (wt/vol) Tris-Glycine gel.

F, Binding characteristics of the neutralizing mAbs determined by using BLI. Recombinant SARS-CoV-2 Omicron BA.1 RBD were covalently immobilized onto a HIS1K sensor, all measurements were performed by using a serial 2-fold dilution of purified mAbs, starting from 50 nM (Magenta) to 1.56 nM (Brown). Global fit curves are shown as red dashed lines, The vertical black dotted dashed lines indicate the transition between association and disassociation phases.

Figure S2

Memory B

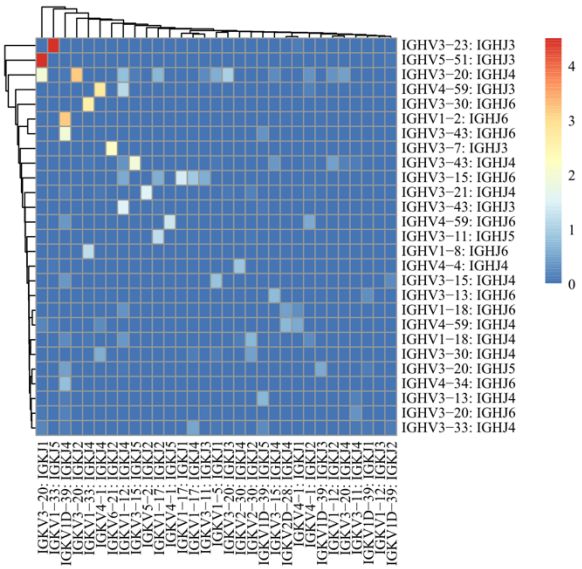

PBMC

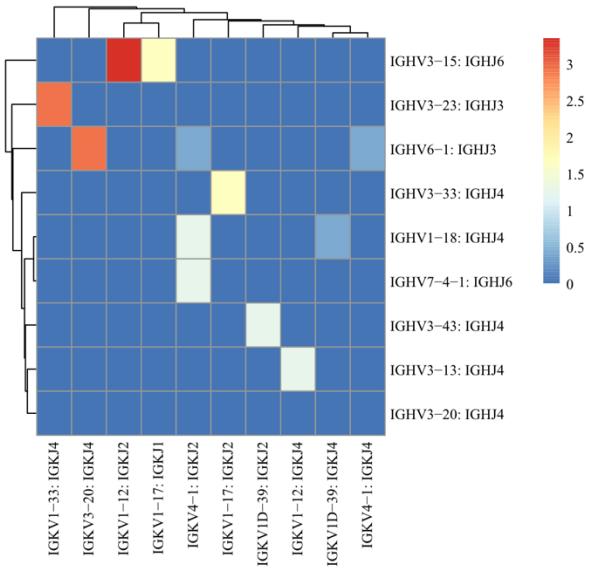

Plasma B

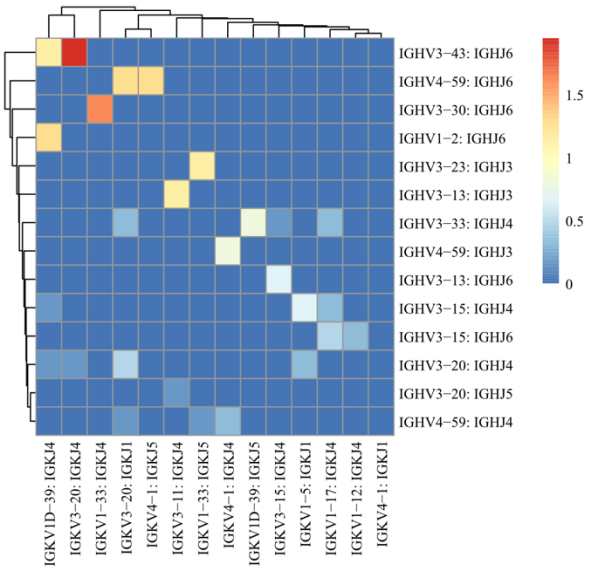

Figure S2. Heatmaps for non-stochastic paired BCR repertoire, Related to Figures 1 and 2

Heatmaps showing the paired of immunoglobin heavy chains and light chains gene variable region segment of clonotypes in Omicron BA.1-RAMIHM mouse. The reader color means the percentage of higher usage of specific VH-VL gene pairs. Memory B library, Plasma B library and PBMC library were shown in separate plots.

Source data and additional statistics for experiments are in supplemental excel file(s).

Figure S3

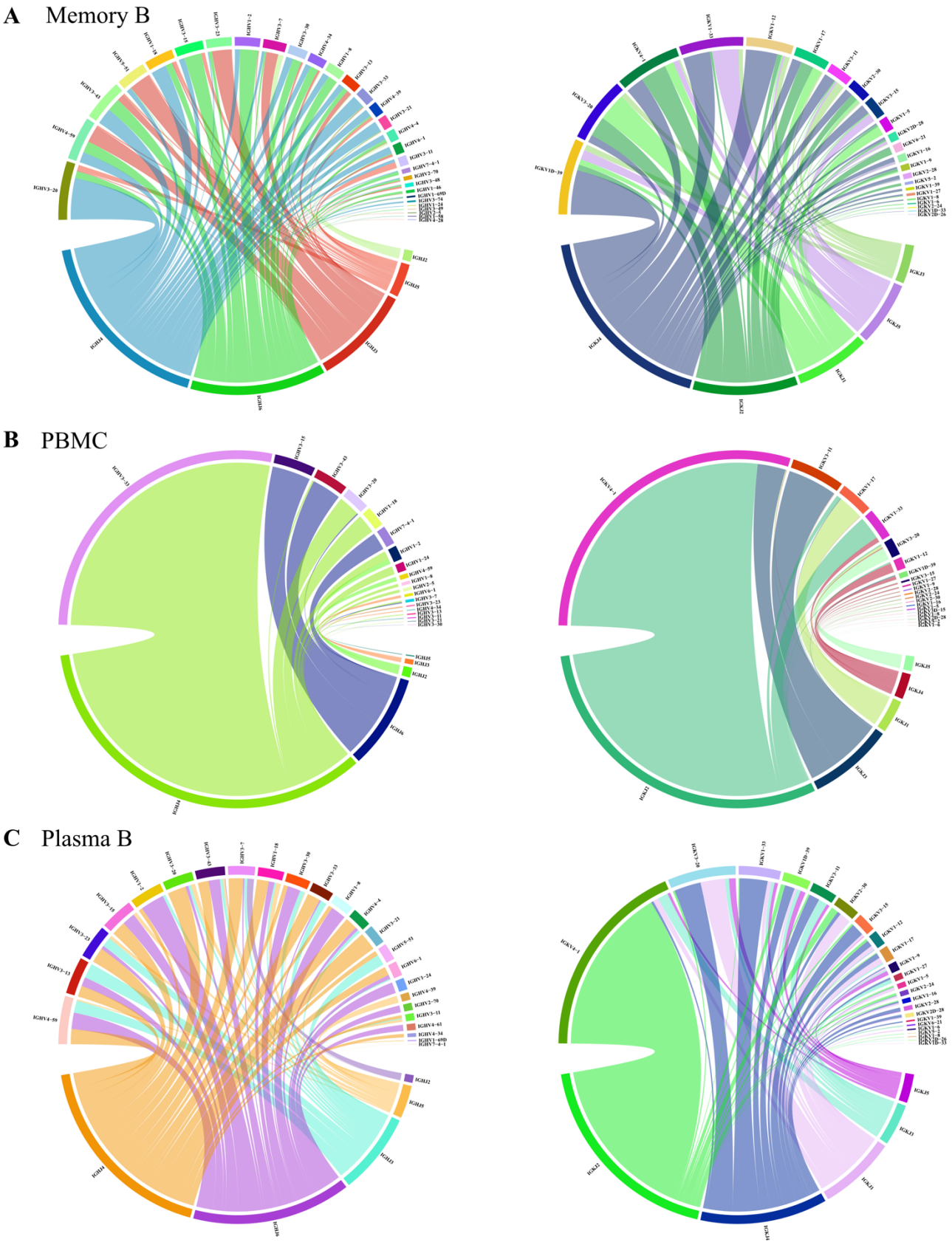

Figure S3. Distribution of heavy- and light- chain V/J segment recombination in Omicron BA.1-RAMIHM mouse, Related to Figures 1 and 2

Chord diagrams (circos plots) showing the distribution of all heavy- and light-chain V and J gene-segment recombination obtained in each representative library. Interconnecting lines indicate the relationship between antibodies that share V and J gene-segment at both IGH and IGL.

A. Memory B library,

B. PBMC library,

C. Plasma B library.

Source data and additional statistics for experiments are in supplemental excel file(s).

Figure S4

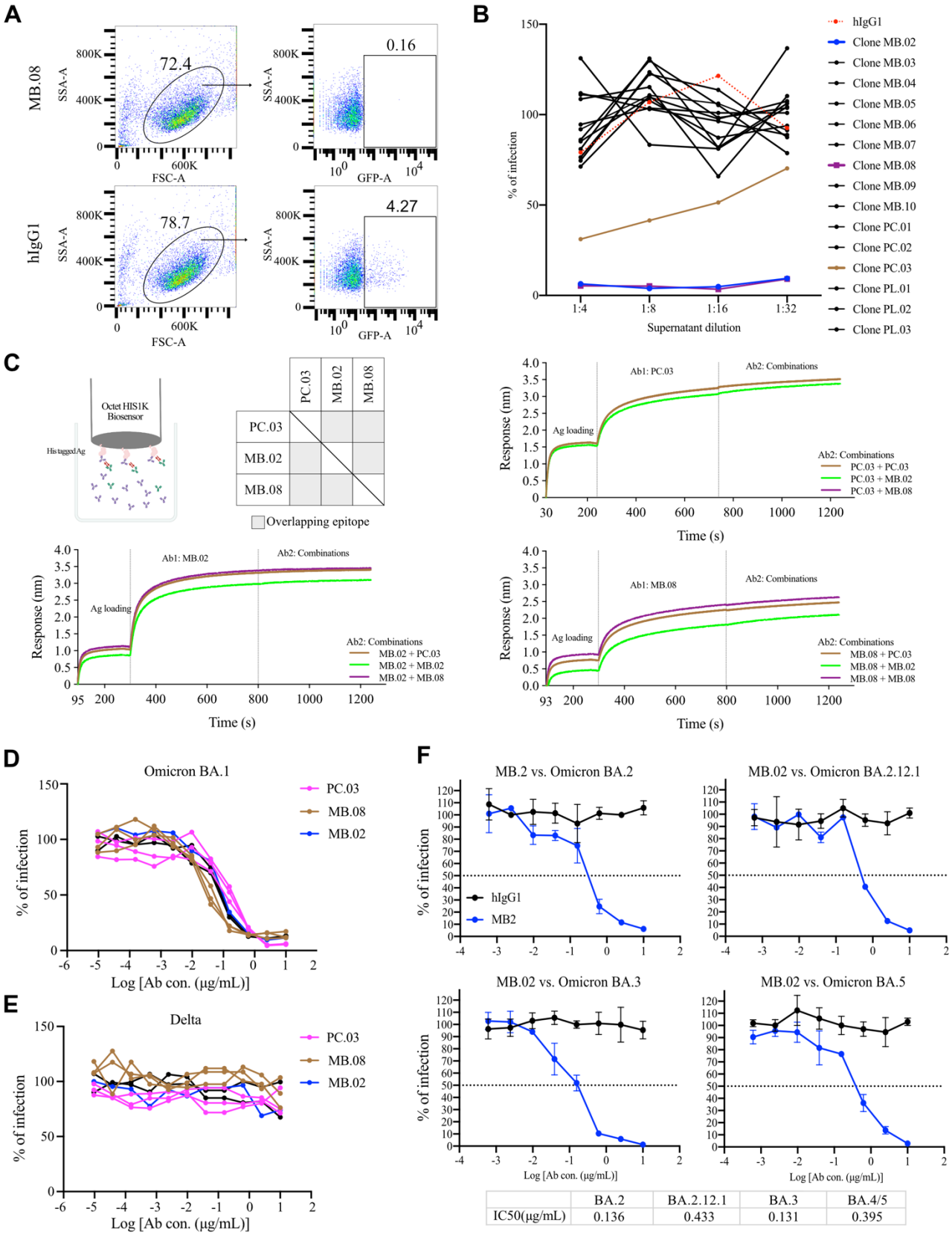

	BA.2	BA.2.12.1	BA.3	BA.4/5
IC50(μg/mL)	0.136	0.433	0.131	0.395

41

Figure S4. Neutralizing abilities and epitope binning of the potent neutralizing mAbs, Related to Figure 2

A, Gating strategy used for GFP-based neutralization analysis.

B, Neutralization potency measured by using a pseudovirus neutralization assay. Data for each mAb were obtained from a representative neutralization experiment, which contains three replicates. Data are graphed as percentage neutralization relative to virus-only infection control.

C, Schematic of epitope binning experiment. Summary data of BLI (C) results. The matrix presents the concluded epitope specificity for each competition experiments. The column indicated the primary loading antibody, and the row indicated the secondary antibody combinations. Epitope binning of the three potent neutralizing mAbs. Sensorgram show distinct binding patterns when pairs of testing antibodies were sequentially applied to the recombinant SARS-CoV2 Omicron BA.1 RBD covalently immobilized onto a HIS1K sensor. The level of increment in response unit comparing with or without prior antibody incubation is the key criteria for determining the two mAbs recognize the separate or closely situated epitopes.

D, Individual neutralization curves for leading Omicron mAbs against Omicron BA.1 pseudovirus.

E, Individual neutralization curves for leading Omicron mAbs against Delta pseudovirus.

F, MB.02 neutralizes spike-coated pseudoviruses of currently circulating Omicron sublineages. The graph presents the normalized GFP signals for detection of HEK293T-ACE2 cells, 24 h after infection with pseudovirus of currently circulating Omicron sublineages, in the presence of increasing concentration of indicated Omicron mAb.

Source data and additional statistics for experiments are in supplemental excel file(s).

Figure S5

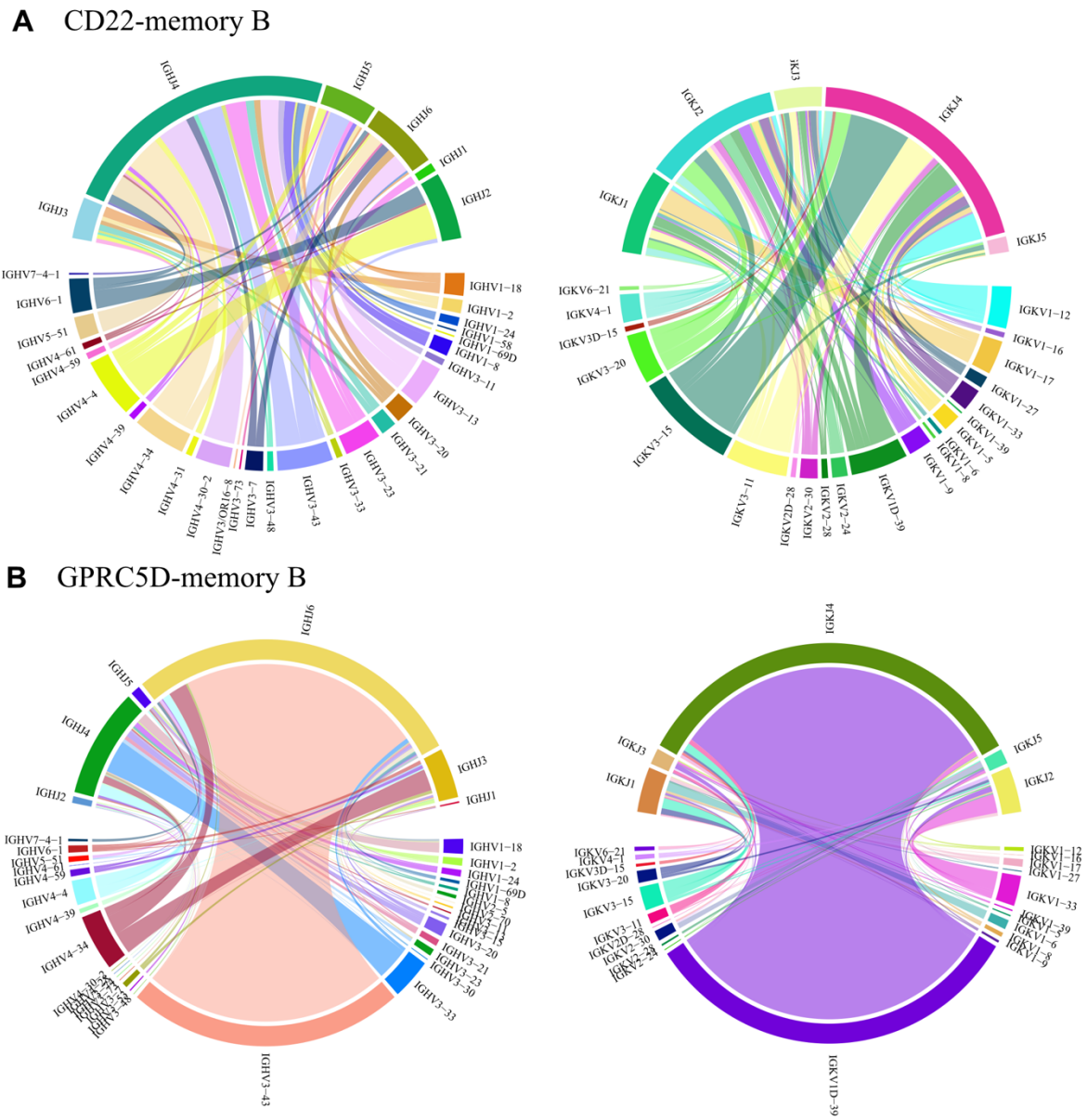
A CD22-memory B
IGHJ4
IGHJ5
IGHJ6
IGHJ1
IGHJ2
IGHJ3
IGHV7-4-1
IGHV6-1
IGHV5-51
IGHV4-61
IGHV4-59
IGHV4-4
IGHV4-39
IGHV4-34
IGHV4-31
IGHV4-30-2
IGHV3OR16-8
IGHV3-23
IGHV3-7
IGHV3-48
IGHV3-43
IGHV3-33
IGHV3-23
IGHV3-21
IGHV3-20
IGHV3-13
IGHV3-11
IGHV1-8
IGHV1-69D
IGHV1-58
IGHV1-24
IGHV1-2
IGHV1-18
IGKJ3
IGKJ2
IGKJ4
IGKJ1
IGKJ5
IGKV6-21
IGKV4-1
IGKV3D-15
IGKV3-20
IGKV3-15
IGKV3-11
IGKV2D-28
IGKV2-30
IGKV2-28
IGKV2-24
IGKV1D-39
IGKV1-9
IGKV1-8
IGKV1-6
IGKV1-5
IGKV1-39
IGKV1-33
IGKV1-27
IGKV1-17
IGKV1-16
IGKV1-12
B GPRC5D-memory B
IGHJ6
IGHJ5
IGHJ4
IGHJ2
IGHJ3
IGHJ1
IGHV7-4-1
IGHV6-1
IGHV5-51
IGHV4-61
IGHV4-59
IGHV4-4
IGHV4-39
IGHV4-34
IGHV3-43
IGHV3-33
IGHV3-30
IGHV3-23
IGHV3-21
IGHV3-20
IGHV1-69D
IGHV1-24
IGHV1-2
IGHV1-18
IGKJ4
IGKJ3
IGKJ1
IGKJ5
IGKJ2
IGKV6-21
IGKV4-1
IGKV3D-15
IGKV3-20
IGKV3-15
IGKV3-11
IGKV2D-28
IGKV2-30
IGKV2-28
IGKV2-24
IGKV1D-39
IGKV1-33
IGKV1-27
IGKV1-17
IGKV1-16
IGKV1-12

63

Figure S5. Distribution of heavy- and light- chain V/J segment recombination in TAA-RAMIHM mice, Related to Figures 3 and 4

A, Chord diagrams (circos plots) showing the distribution of all heavy- and light-chain V and J gene-segment recombination obtained from CD22 memory B cell library. Interconnecting lines indicate the relationship between antibodies that share V and J gene-segment at both IGH and IGL.

B, Chord diagrams (circos plots) showing the distribution of all heavy- and light-chain V and J gene-segment recombination obtained from GPRC5D memory B cell library. Interconnecting lines indicate the relationship between antibodies that share V and J gene-segment at both IGH and IGL.

Figure S6

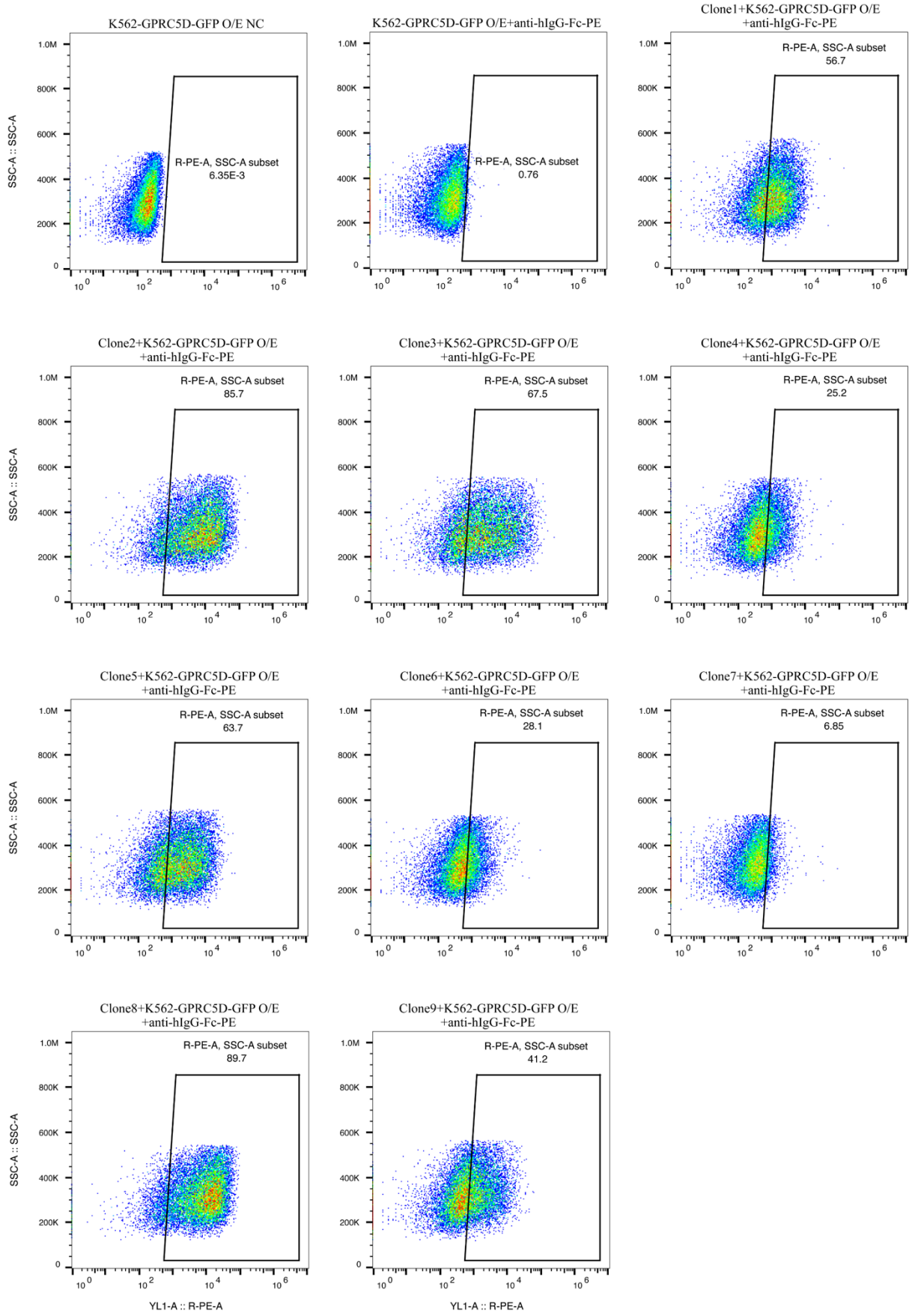
K562-GPRC5D-GFP O/E NC
R-PE-A, SSC-A subset
6.35E-3
K562-GPRC5D-GFP O/E+anti-hIgG-Fc-PE
R-PE-A, SSC-A subset
0.76
Clone1+K562-GPRC5D-GFP O/E
+anti-hIgG-Fc-PE
R-PE-A, SSC-A subset
56.7
Clone2+K562-GPRC5D-GFP O/E
+anti-hIgG-Fc-PE
R-PE-A, SSC-A subset
85.7
Clone3+K562-GPRC5D-GFP O/E
+anti-hIgG-Fc-PE
R-PE-A, SSC-A subset
67.5
Clone4+K562-GPRC5D-GFP O/E
+anti-hIgG-Fc-PE
R-PE-A, SSC-A subset
25.2
Clone5+K562-GPRC5D-GFP O/E
+anti-hIgG-Fc-PE
R-PE-A, SSC-A subset
63.7
Clone6+K562-GPRC5D-GFP O/E
+anti-hIgG-Fc-PE
R-PE-A, SSC-A subset
28.1
Clone7+K562-GPRC5D-GFP O/E
+anti-hIgG-Fc-PE
R-PE-A, SSC-A subset
6.85
Clone8+K562-GPRC5D-GFP O/E
+anti-hIgG-Fc-PE
R-PE-A, SSC-A subset
89.7
Clone9+K562-GPRC5D-GFP O/E
+anti-hIgG-Fc-PE
R-PE-A, SSC-A subset
41.2
SSC-A :: SSC-A
YL1-A :: R-PE-A

73

Figure S6. Validation of individual clones of mAbs's binding against GPRC5D-overexpressed K562 cells, Related to Figure 4

Flow cytometry plots of individual clones of RAMIHM-generated human GPRC5D mAbs's binding against GPRC5D-overexpressed K562 cells.

Figure S7

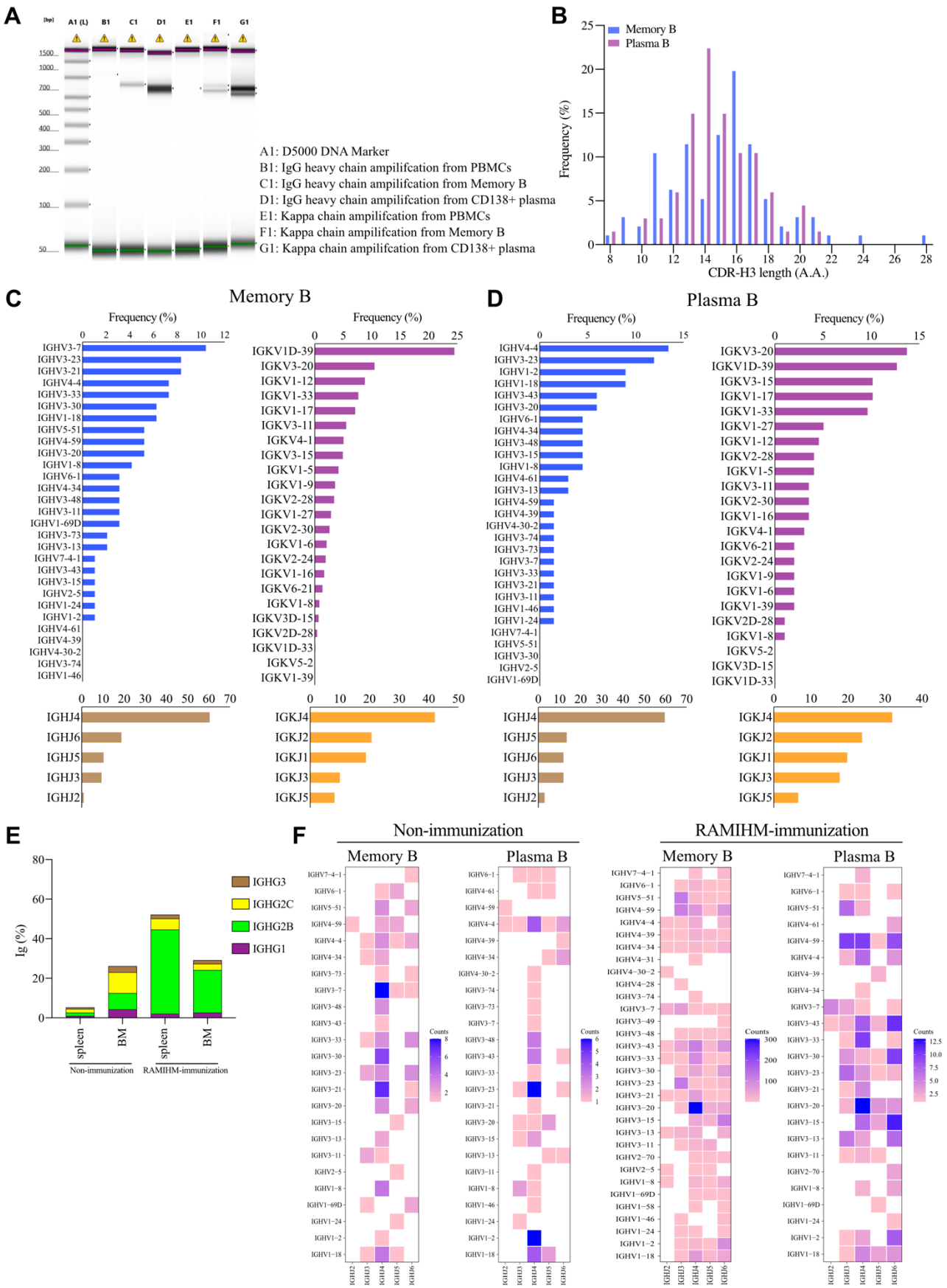
A
A1 (L)
B1
C1
D1
E1
F1
G1
A1: D5000 DNA Marker
B1: IgG heavy chain ampilifcation from PBMCs
C1: IgG heavy chain ampilifcation from Memory B
D1: IgG heavy chain ampilifcation from CD138+ plasma
E1: Kappa chain ampilifcation from PBMCs
F1: Kappa chain ampilifcation from Memory B
G1: Kappa chain ampilifcation from CD138+ plasma
B
Memory B
Plasma B
Frequency (%)
CDR-H3 length (A.A.)
C
Memory B
D
Plasma B
Frequency (%)
E
Ig (%)
IGHG3
IGHG2C
IGHG2B
IGHG1
spleen
BM
Non-immunization
RAMIHM-immunization
F
Non-immunization
RAMIHM-immunization
Memory B
Plasma B
Counts

Figure S7. Natural B cell levels in non-immunized humanized mouse, Related to Figures 1, 3, 4

A, Single cell BCR libraries construction from non-immunized humanized mouse. PCR products from Memory B library, Plasma B library and PBMC library were loaded in separate lanes.

B. Distribution of heavy chain complementarity-determining region 3 (HCDR3) length in memory B cells and plasma B cells from non-immunized humanized mouse.

C, Global frequencies of IGHV, IGHJ, IGKV, and IGKJ genes usage in memory B cells from non-immunized humanized mouse.

D, Global frequencies of IGHV, IGHJ, IGKV, and IGKJ genes usage in plasma B cells from non-immunized humanized mouse.

E, Antibody isotype switching was induced by Omicron BA.1-RAMIHM.

F, Rapid antibody clonal expansion and diversification were elevated by Omicron BA.1-RAMIHM.